ORIGINAL RESEARCH

Novel Loss-of-Function *KCNA5* Variants in Pulmonary Arterial Hypertension

Alba Vera-Zambrano[1,2,3], Mauro Lago-Docampo[4,5], Natalia Gallego[6,7,8], Juan Felipe Franco-Gonzalez[9], Daniel Morales-Cano[10,11], Alejandro Cruz-Utrilla[12,13], Marta Villegas-Esguevillas[1,14,15], Edgar Fernández-Malavé[16,17], Pilar Escribano-Subías[12,13], Jair Antonio Tenorio-Castaño[6,7,8], Francisco Perez-Vizcaino[1,14,15], Diana Valverde[4,5], Teresa González[2,3], Spanish group of Ion Channels in Pulmonary Hypertension (SICPH) investigators[1,2,4,6,13,14], and Angel Cogolludo[1,14,15]

[1]Department of Pharmacology and Toxicology and [16]Department of Immunology, Ophthalmology and ENT, School of Medicine, University Complutense of Madrid, Madrid, Spain; [2]Department of Biochemistry, School of Medicine, University Autonoma of Madrid, Madrid, Spain; [3]Instituto de Investigaciones Biomédicas "Alberto Sols" Consejo Superior de Investigaciones Científicas-Universidad Autónoma de Madrid, Madrid, Spain; [4]Centro de Investigación en Nanomateriais e Biomedicina (CINBIO), Universidade de Vigo, Vigo, Spain; [5]Rare Diseases and Pediatric Medicine, Galicia Sur Health Research Institute, SERGAS-UVIGO, Vigo, Spain; [6]Institute of Medical and Molecular Genetics-IdiPAZ, Universitary Hospital La Paz, University Autonoma of Madrid, Madrid, Spain; [7]Centro de Investigación Biomédica en Red de Enfermedades Raras, Instituto de Salud Carlos III, Madrid, Spain; [8]ITHACA, European Reference Network on Rare Congenital Malformations and Rare Intellectual Disability, University Hospital La Paz, Madrid, Spain; [9]Department of Structural and Chemical Biology, Margarita Salas Center for Biological Research, Scientific Research Council, Madrid, Spain; [10]Experimental Pathology of Atherosclerosis Laboratory, National Center for Cardiovascular Research Carlos III, Madrid, Spain; [11]Atherosclerosis Research Unit, Department of Clinical Medicine, Aarhus University, Aarhus, Denmark; [12]Centro de Investigación Biomédica en Red de Enfermedades Cardiovasculares, and [14]Centro de Investigación Biomédica en Red de Enfermedades Respitatorias, Instituto de Salud Carlos III, Madrid, Spain; [13]Unidad Multidisciplinar de Hipertensión Pulmonar, Servicio de Cardiología, Hospital Universitario 12 de Octubre, Madrid, Spain; [15]Instituto de Investigación Sanitaria Gregorio Marañón, Madrid, Spain; and [17]Instituto de Investigación Sanitaria Hospital 12 de Octubre, Madrid, Spain

ORCID IDs: 0000-0002-4040-1920 (A.V.-Z.); 0000-0002-8799-6079 (M.L.-D.); 0000-0002-1692-4633 (D.M.-C.); 0000-0002-3851-4037 (A.C.-U.); 0000-0001-6309-7418 (F.P.-V.); 0000-0002-1382-1698 (A.C.).

Abstract

Reduced expression and/or activity of Kv1.5 channels (encoded by *KCNA5*) is a common hallmark in human or experimental pulmonary arterial hypertension (PAH). Likewise, genetic variants in *KCNA5* have been found in patients with PAH, but their functional consequences and potential impact on the disease are largely unknown. Herein, this study aimed to characterize the functional consequences of seven *KCNA5* variants found in a cohort of patients with PAH. Potassium currents were recorded by patch-clamp technique in HEK293 cells transfected with wild-type or mutant Kv1.5 cDNA. Flow cytometry, Western blot, and confocal microscopy techniques were used for measuring protein expression and cell apoptosis in HEK293 and human pulmonary artery smooth muscle cells. *KCNA5* variants (namely, Arg184Pro and Gly384Arg) found in patients with PAH resulted in a clear loss of potassium channel function as assessed by electrophysiological and molecular modeling analyses. The Arg184Pro variant also resulted in a pronounced reduction of Kv1.5 expression. Transfection with Arg184Pro or Gly384Arg variants decreased apoptosis of human pulmonary artery smooth muscle cells compared with the wild-type cells, demonstrating that *KCNA5* dysfunction in both variants affects cell viability. Thus, in addition to affecting channel activity, both variants were associated with impaired apoptosis, a crucial process linked to the disease. The estimated prevalence of dysfunctional *KCNA5* variants in the PAH population analyzed was around 1%. The data indicate that some *KCNA5* variants found in patients with PAH have critical consequences for channel function, supporting the idea that *KCNA5* pathogenic variants may be a causative or contributing factor for PAH.

Keywords: *KCNA5* variants; Kv1.5; pulmonary hypertension; ion channels; potassium channels

(Received in original form June 14, 2022; accepted in final form March 14, 2023)

Supported by the Fundación Contra la Hipertensión Pulmonar; Ministerio de Ciencia e Innovación (PID2020-117939RB-I00 to A.C., PID2019-104366RB-C21 to T.G., and PID2019-107363RB-I00 to F.P.-V.); Comunidad de Madrid (B2017/BMD-3727 to A.C.) and Instituto de Salud Carlos III (PI18/01233 and PI21/01593), with funds from the European Union (Fondo Europeo de Desarrollo Regional); an annual grant from the Federación Española de Enfermedades Raras; predoctoral fellowships from La Universidad Autónoma de Madrid, Xunta de Galicia (ED481A-2018/304), and the Complutense University of Madrid to A.V.-Z., M.L.-D., and M.V.-E., respectively; and a research-training contract "Rio Hortega" (CM20/00164) from the Spanish Ministry of Science and Innovation (Instituto de Salud Carlos III) (to A.C.-U.).

Am J Respir Cell Mol Biol Vol 69, Iss 2, pp 147–158, August 2023

Originally Published in Press as DOI: 10.1165/rcmb.2022-0245OC on March 14, 2023
Internet address: www.atsjournals.org

Clinical Relevance

Here, we show that some *KCNA5* variants found in pulmonary arterial hypertensive patients have critical consequences for channel function. Our data support the idea that *KCNA5* pathogenic variants may be a causative or contributing factor for this disease.

Pulmonary arterial hypertension (PAH) is a rare, debilitating, and progressive disease defined by the sustained elevation of the mean pulmonary artery pressure and the pulmonary vascular resistance above 20 mm Hg and 3 Wood units at rest, respectively. The chronic elevation of pulmonary pressures leads to right ventricular and heart failure and, eventually, to transplantation or death, if untreated (1). PAH has complex and multifactorial pathogenesis attributed to persistent vasoconstriction and pulmonary vascular remodeling characterized by pulmonary artery smooth muscle cell (PASMC) hypertrophy and progressive neointimal proliferation of endothelial cells, leading to occlusive vascular lesions of the smallest pulmonary arteries (1, 2). Pulmonary vascular remodeling in PAH results from an imbalance between smooth muscle cell growth and apoptosis, caused by increased PASMC proliferation and/or decreased PASMC apoptosis (3–5).

There is growing evidence that K^+ channel dysfunction critically contributes to excessive vasoconstriction and inappropriate pulmonary vascular remodeling in PAH (6, 7). In PASMCs, K^+ channels are responsible for setting resting membrane potential (6, 8, 9) and thus regulating pulmonary vascular tone, cell apoptosis, proliferation, and survival (3). Their activation produces membrane hyperpolarization, which precludes the opening of voltage-gated L-type Ca^{2+} channels, leading to vasodilation. On the other hand, reduced K^+ conductance produces depolarization, which enhances voltage-gated L-type Ca^{2+} channel opening, leading to vasoconstriction and proliferation. Additionally, K^+ channels have been implicated in both the early and late stages of apoptosis. In this regard, K^+ is the dominant cation in the cytoplasm and thus plays an important role in maintaining cell volume. Therefore, in early apoptosis, reduced K^+ channel activity inhibits apoptotic cell shrinkage, and in later stages of apoptosis, it decreases caspase activation and DNA fragmentation (4, 10).

In PAH, the downregulation of K^+ channels, particularly Kv1.5 and TASK-1, is considered an early contributor to the pathophysiology of the disease (6, 8, 9, 11–16). Reduced expression of Kv1.5 has been considered a potential target in either human or experimental PAH (9, 11, 13, 17–19). In addition, different pathogenic variants or polymorphisms in genes encoding K^+ channels (*KCNK3*, *KCNJ8*, and *ABCC8/9*) and SNPs in *KCNA5* have been previously related to the disease (6, 12, 15, 20, 21). Nevertheless, *KCNA5* is among the genes related to PAH with a lower level of evidence to play a causal role (22–24), mainly because of the limited functional studies available.

Herein, we have functionally characterized seven *KCNA5* variants described in Spanish patients with PAH. Our study identifies novel loss-of-function *KCNA5* mutations, providing crucial information to consider *KCNA5* dysfunction a risk factor for PAH and an attractive pharmacological target.

Methods

An extended version of the materials and methods is available in the data supplement.

Patients

Patients were recruited from the Spanish PAH registries (REHIPED and REHAP); all index cases or legal tutors gave their consent to participate in this project, and the investigation was conducted in accordance with the Declaration of Helsinki. This project was approved by the ethical committees of clinical research of Galicia, the Hospital Universitario La Paz, and the Hospital Universitario 12 de Octubre (PI-1210 and PI18/01233).

Variant Selection

We performed a genetic analysis through a customized massive parallel sequencing panel. We selected several changes in the *KCNA5* gene described in a Spanish cohort of patients with PAH (20, 22). For the functional analysis, we focused on those variants that, on the basis of guidelines from the American College of Medical Genetics (ACMG), were not classified as benign (*see* Table E1 in the data supplement). From the variants detected, we did not analyze two variants—p.Leu316Alafs*142, a large frameshift variant, and p.Glu208*, a deletion removing the entire C terminus—because such structural modifications are incompatible with channel function and were classified as pathogenic by the ACMG guidelines.

Site-Directed Mutagenesis

Site-directed mutagenesis for each of the variants was performed with the hKv1.5-GFPpBK plasmid using the primers listed in Table E2.

Cell Transfection

HEK293 cells, HeLa cells, and human PASMCs (hPASMCs) were transfected with WT or mutant hKv1.5-GFP-pBK channels using Lipofectamine 2000 (Invitrogen) according to the manufacturer's instructions.

Author Contributions: A.C. and A.V.-Z. conceived and designed the research. A.V.-Z., M.L.-D., D.M.-C., M.V.-E., E.F.-M., and F.P.-V. performed the experiments and analyzed the experimental data. J.F.F.-G. and A.V.-Z. performed the computational analysis. N.G., A.C.-U., P.E.-S., and J.A.T.-C. acquired and analyzed the clinical data. P.E.-S., J.A.T.-C., F.P.-V., D.V., T.G., and A.C. interpreted the data. A.V.-Z. and A.C. drafted the manuscript. The SICPH (Spanish group of Ion Channels in Pulmonary Hypertension) investigators assisted in the interpretation and discussion of the data. All authors edited, revised, and approved the final version of the manuscript.

Correspondence and requests for reprints should be addressed to Angel Cogolludo, Ph.D., Department of Pharmacology and Toxicology, School of Medicine, University Complutense of Madrid, Ciudad Universitaria S/N, 28040 Madrid, Spain. E-mail: acogolludo@med.ucm.es.

A complete list of the Spanish Group of Ion Channels in Pulmonary Hypertension (SICPH) investigator members may be found in the data supplement.

This article has a related editorial.

This article has a data supplement, which is accessible from this issue's table of contents at www.atsjournals.org.

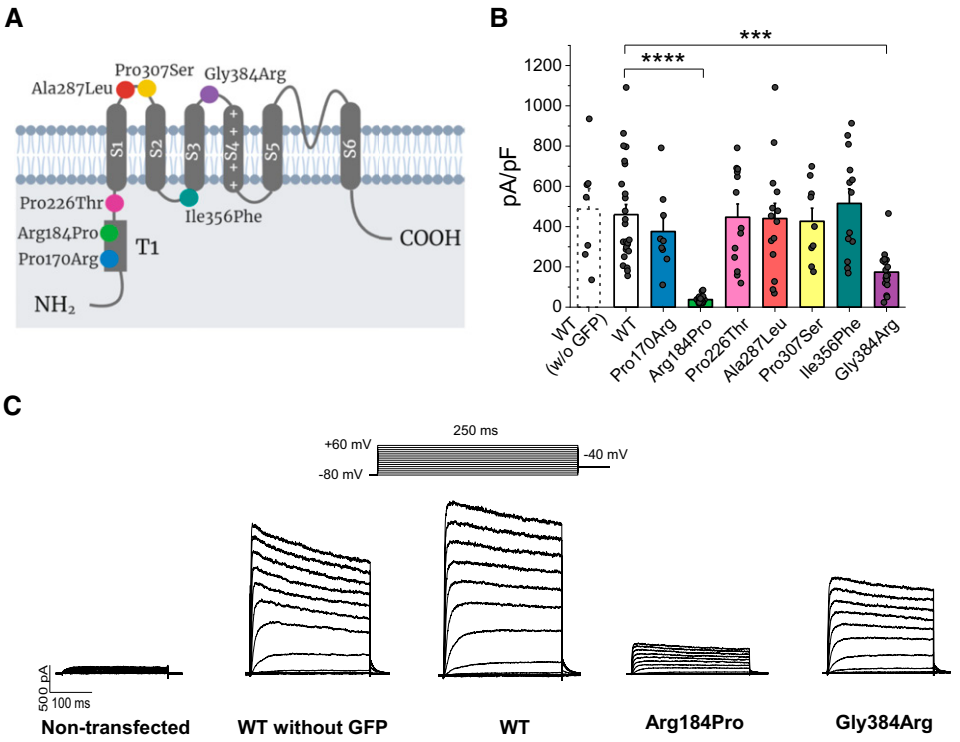

Figure 1. Current amplitude of Kv1.5 channels in seven *KCNA5* variants of patients with pulmonary arterial hypertension recorded in HEK293 cells. (*A*) Schematic diagram of Kv1.5 channel α-subunit showing the six transmembrane domains (S1–S6), the tetramerization domain (T1), and the cytosolic NH_2 and COOH termini. All *KCNA5* variants are labeled with colored dots. Created with biorender.com. (*B*) Maximum current density (in pA/pF) at +40 mV in wild-type (WT) channel with and without fused GFP and seven *KCNA5* variants ($n = 7$–25). Results are presented as mean ± SEM. ***$P < 0.001$ and ****$P < 0.0001$. (*C*) Representative current traces for an endogenous HEK293 current, the WT channel with and without fused GFP, and the Arg184Pro and Gly384Arg variants after applying the protocol shown at the top of the panel. Vertical scale bar: 500 pA; horizontal scale bar: 100 ms. pA/pF = picoamperes per picofarad.

Flow Cytometry

Forty-eight hours after transfection, GFP-positive cells were subjected to fluorescence-activated cell sorting using a 488-nm laser (FACSVantage SE; BD Biosciences). For measuring Kv1.5 protein expression (GFP^+) and cell death (annexin V and propidium iodide staining), cells were analyzed on a FACSCanto II cytometer (BD Biosciences).

Immunoblot Analysis

Kv1.5 was detected using anti-Kv1.5 APC-150 (1:1,000; Alomone) and a peroxidase-coupled anti-mouse IgG secondary antibody (1:10,000; Santa Cruz Biotechnology). Vinculin was used as a loading control (1:80,000; Santa Cruz Biotechnology).

Electrophysiological Recordings and Data Acquisition

Currents were recorded using the whole-cell patch-clamp technique with a patch-clamp amplifier (Axopatch-200B; Molecular Devices) and stored in a computer by a Digidata 1440A A/D converter (Molecular Devices), as described previously (9, 11).

Immunofluorescence

Transfected HeLa cells were incubated with the anti-pancadherin (1:500; Abcam, #ab22744) and anti-Kv1.5 APC-004 (1:50; Alomone) to stain cell membrane and Kv1.5 channels.

Molecular Modeling

The closed-state model of the Kv1.5 channel was obtained by molecular homology from the crystal structure of Kv1.2 and a subsequent molecular dynamics simulation embedded into a lipid membrane. Mutations were built using the Mutator plugin from VMD software (25). Molecular dynamics simulations for both mutations were performed with QwikMD for each cluster (26). The solvent-accessible surface area (SASA) was analyzed for the wild-type (WT) channel and both mutations using VMD software.

Statistical Analysis

The data are presented as mean ± SEM. Outliers were detected with the ROUT method ($Q = 1$). Comparisons were performed by using a one-way ANOVA followed by a *post hoc* Dunnett test (multiple comparisons) or by a two-tailed unpaired Student's *t* test (comparisons between two groups), and statistical significance was set at $P < 0.05$. All the statistical analysis was conducted using GraphPad Prism 8 (GraphPad Software).

Results

Some *KCNA5* Variants Show an Alteration in the Kv1.5 Channel Function

We performed an electrophysiological characterization by whole-cell patch-clamp of the WT Kv1.5 channel and the *KCNA5* variants of interest to investigate whether the function of the channel was altered

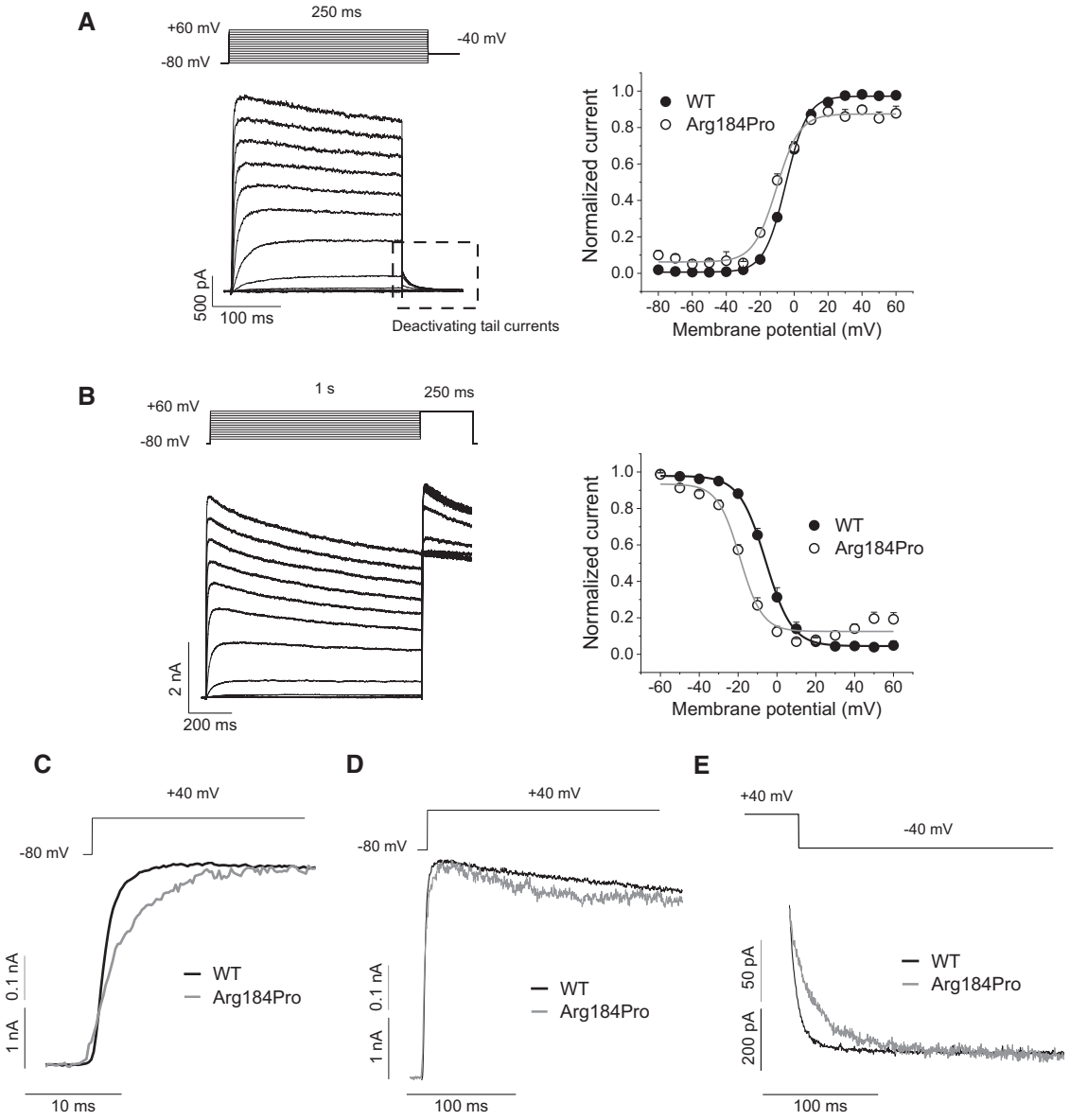

Figure 2. Electrophysiological characterization of Kv1.5 current in WT channel (black) and Arg184Pro variant (gray) recorded in HEK293 cells. (*A*) Left: representative Kv1.5 current traces obtained after applying the voltage protocol shown at the top of the panel. Vertical scale bar: 500 pA; horizontal scale bar: 100 ms. Right: normalized activation curves of WT Kv1.5 ($n = 16$) and Arg184Pro variant ($n = 9$). Maximum deactivating tail currents recorded by repolarization to −40 mV (highlighted by the square of dashed lines) were plotted versus the membrane potential of the previous pulse and fitted to a Boltzmann equation to obtain the E_h and s values. (*B*) Left: representative Kv1.5 current traces obtained after applying the voltage protocol shown at the top of the panel. Vertical scale bar: 500 pA; horizontal scale bar: 100 ms. Right: normalized inactivation curves of WT Kv1.5 ($n = 14$) and Arg184Pro variant ($n = 14$) obtained after plotting maximum current amplitude recorded at +60 mV versus the membrane potential of the previous pulse and fitted to a Boltzmann equation to obtain the E_h and s values. In (*A*) and (*B*), results are presented as mean ± SEM. (*C–E*) Activation kinetics (*C*), inactivation kinetics (*D*), and deactivation kinetics (*E*) showing representative current traces of WT Kv1.5 channel (black) and Arg184Pro variant (gray). Recordings in (*C*) and (*D*) are from the same experiment but with different time scales. In (*C–E*), normalized current traces are shown to facilitate the comparison between conditions. Protocols are shown at the top of the panels. In (*C*), vertical scale bars: 0.1 nA (top) and 1 nA (bottom); horizontal scale bar, 10 ms. In (*D*), vertical scale bars: 0.1 nA (top) and 1 nA (bottom); horizontal scale bar, 100 ms. In (*E*), vertical scale bars: 50 pA (top) and 200 pA (bottom); horizontal scale bar, 100 ms.

(Figure 1A and Table E3). A macroscopic Kv1.5 current was observed in WT channel–transfected cells in contrast with nontransfected HEK cells. This was comparable with that observed in Kv1.5 channels not fused with GFP (Figures 1B and 1C). Kv1.5 current amplitude was also recorded in cells transfected with the different variants and expressed as current density (in picoamperes per picofarad), showing a clear decrease in Gly384Arg and especially in Arg184Pro (Figure 1B and

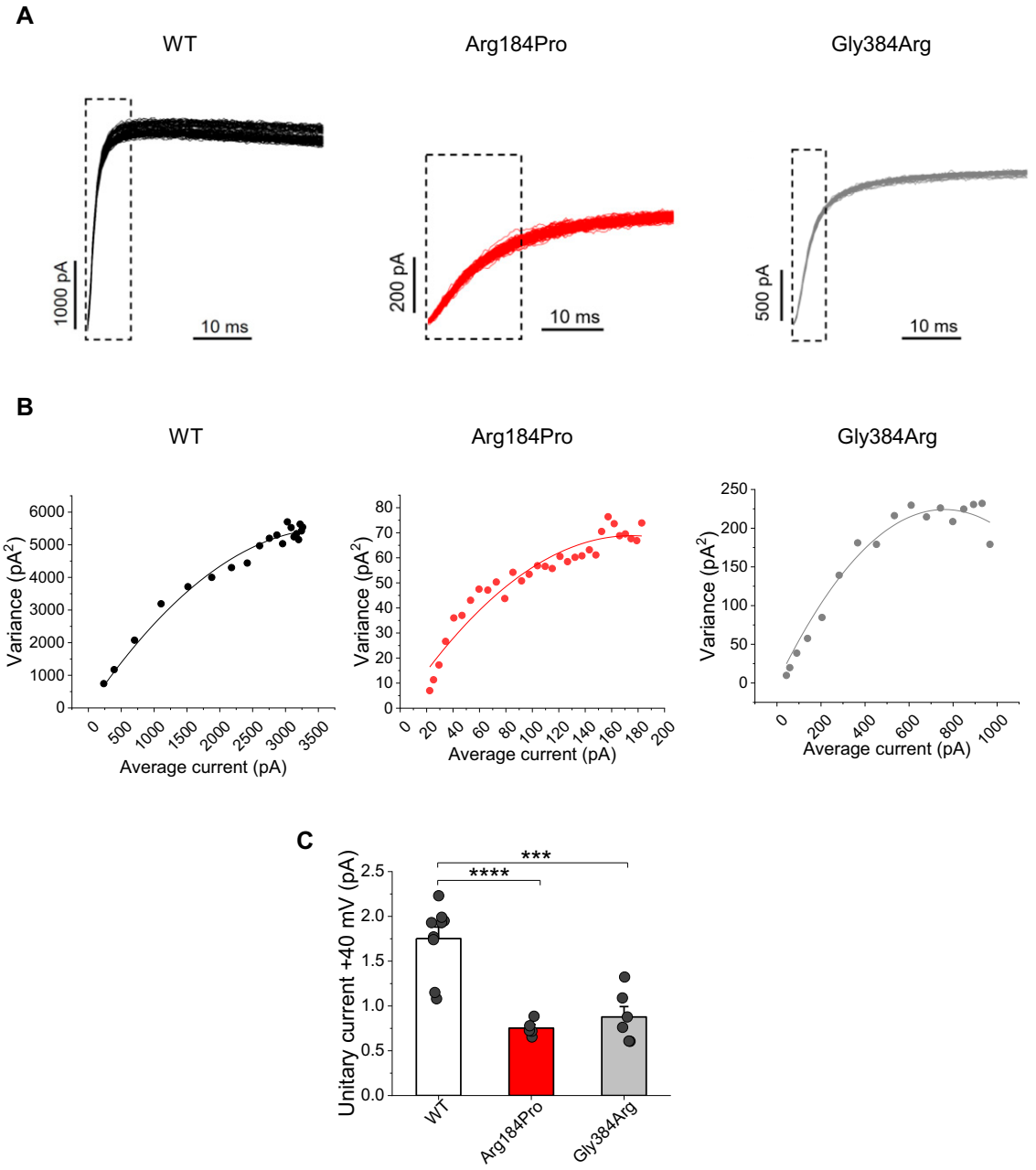

Figure 3. Unitary current is reduced in Arg184Pro and Gly384Arg variants. (*A*) Original recordings of cells transfected with WT channel, Arg184Pro, and Gly384Arg held at −80 mV and pulsed 100 times to +40 mV. Scale bars, 100 ms. (*B*) Representative nonstationary noise analysis from WT, Arg184Pro, and Gly384Arg Kv1.5 currents. (*C*) Unitary current measured at +40 mV in WT channel ($n = 9$) and in Arg184Pro ($n = 5$), and Gly384Arg ($n = 6$) variants. Results are presented as mean ± SEM. ***$P < 0.001$ and ****$P < 0.0001$.

Table E3). Figure 1C shows representative current traces of the Kv1.5 current recorded in cells expressing the WT channel or the Arg184Pro and Gly384Arg variants.

In addition to the current amplitude, other electrophysiological characteristics were studied to analyze whether the variants were associated with changes in channel gating (*see* Table E3). Focusing on Arg184Pro, a clear impairment in channel gating properties was found, with a significant leftward shift in the activation (Figure 2A) and inactivation (Figure 2B) curves toward more electronegative values (activation half-maximal voltage [E_h] = –4.91 ± 0.97 mV vs. –9.94 ± 1.37 mV, $n = 16$–20, $P < 0.01$; and inactivation E_h = –5.61 ± 1.69 mV vs. –19.09 ± 1.24 mV, $n = 14$, $P < 0.0001$; for WT Kv1.5 and Arg184Pro, respectively; *see* Table E3). Moreover, slower activation and deactivation kinetics and faster inactivation kinetics were found (Figures 2C–2E and Table E3). In the case of Gly384Arg, a slower activation kinetic was observed (2.8 ± 0.32 ms vs. 1.78 ± 0.09 ms, $n = 15$–20, respectively; $P < 0.05$; *see* Figure E1A and Table E3).

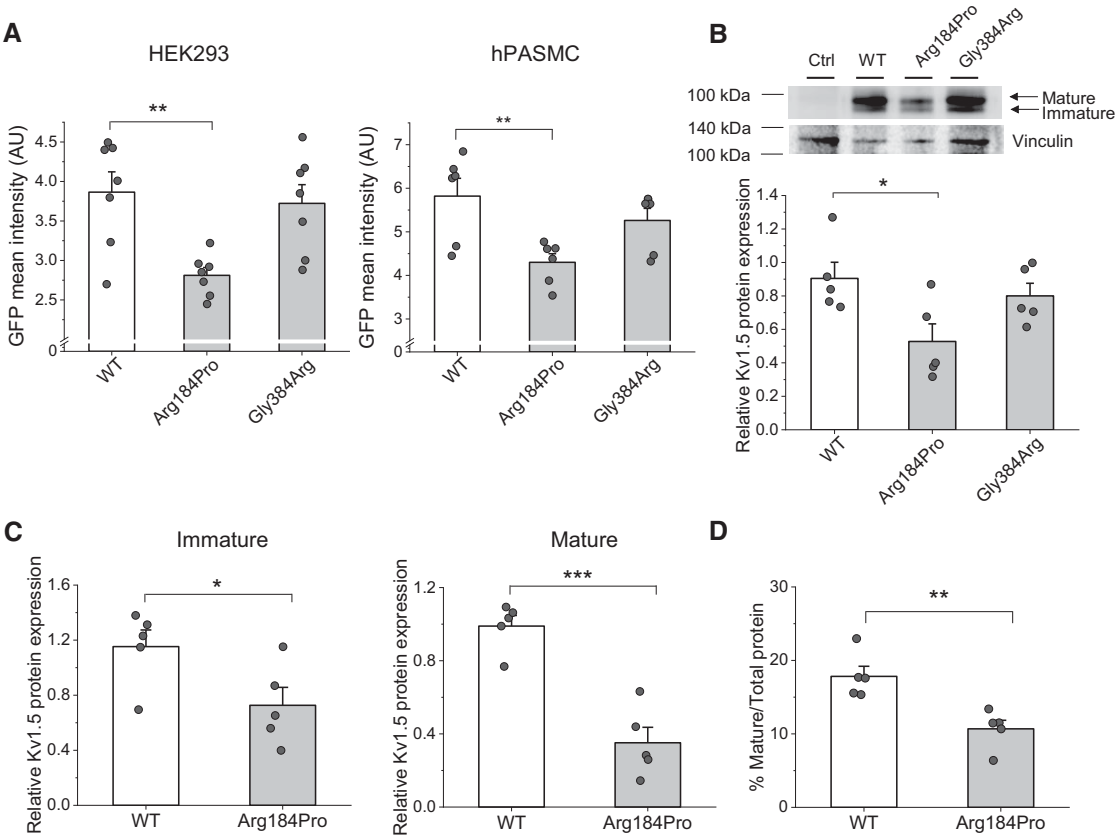

Figure 4. Total Kv1.5 protein expression in WT channel and in Arg184Pro and Gly384Arg variants. (*A*) GFP mean intensity by flow cytometry in HEK293 cells ($n = 7$) and hPASMCs ($n = 6$). (*B*) Relative Kv1.5 protein expression by Western blot probed with an anti-Kv1.5 antibody ($n = 5$) and normalized by vinculin expression in HEK293 cells. The Ctrl corresponds to nontransfected HEK293 cells. (*C*) Relative Kv1.5 protein expression of mature and immature Kv1.5 isoforms in WT channel and Arg184Pro variant ($n = 5$). (*D*) Percentage of mature protein relative to the total protein expression in each condition ($n = 5$). Results are presented as mean ± SEM. $^*P < 0.05$, $^{**}P < 0.01$, and $^{***}P < 0.001$. Ctrl = control; hPASMCs = human pulmonary artery smooth muscle cells.

Moreover, although the Ile356Phe variant did not significantly affect the current amplitude, it resulted in a much slower deactivation kinetic ($\tau_s = 56.66 \pm 3.72$ ms and $\tau_f = 15.01 \pm 1.15$ ms, $n = 12$; vs. $\tau_s = 39.54 \pm 1.53$ ms and $\tau_f = 9.95 \pm 0.69$ ms, $n = 19$ in the WT Kv1.5 channel; $P < 0.001$; *see* Figure E1B and Table E3).

We also calculated the unitary Kv1.5 current for WT, Arg184Pro, and Gly384Arg channels by noise fluctuation analysis (Figures 3A and 3B). We found that the estimated unitary Kv1.5 current was reduced in Arg184Pro and Gly384Arg variants compared with that in WT channels (Figure 3C). The calculated Kv1.5 unitary conductance at +40 mV was 13.27 ± 0.98 pS for the WT channel, 5.70 ± 0.29 pS for Arg184Pro ($P < 0.0001$ vs. WT channel), and 6.75 ± 1.17 pS for Gly384Arg ($P < 0.001$ vs. WT channel). The unitary conductance for WT Kv1.5 channels was comparable with that previously reported using noise fluctuation analysis (27) or single-channel recording (28).

Arg^{184} and Gly^{384} Residues Are Highly Conserved

Multiple sequence alignments were performed in the regions flanking the mutated amino acids Arg^{184} and Gly^{384}. The Arg184Pro mutation is located at the tetramerization domain of the channel (29). This region of shaker-like proteins is highly preserved across animal species from sea anemones to mammals and in the human Kv1.1-Kv1.6 channels (*see* Figures E2 and E3). Only basic amino acids such as arginine or lysine, are allowed in this position. Therefore, substitution for a proline, as in the Arg184Pro mutants, is expected to severely affect channel function. The Gly384Arg mutation is located at an extracellular loop, near the S4 segment. The region flanking this amino acid is relatively preserved among mammals (Figures E3 and E4). However, the Gly^{384} was absent in nonmammal vertebrates, and the homology is completely lost in this region for invertebrates. Partial homology was found with the human Kv1.6 channel and, to a lesser extent, with Kv1.4. These data are consistent with a moderate effect of this mutation on channel function.

Arg184Pro *KCNA5* Variant Results in a Lower Expression of the Channel

We addressed whether the decrease in current amplitude observed in Arg184Pro and Gly384Arg variants could be associated with differences in Kv1.5 expression. Thus, total Kv1.5 protein expression was analyzed by flow cytometry and Western blot. The cytometry analysis revealed a clear reduction of Kv1.5 expression in HEK293 (Figure 4A, left) and hPASMCs (Figure 4A, right) transfected with Arg184Pro, but not in

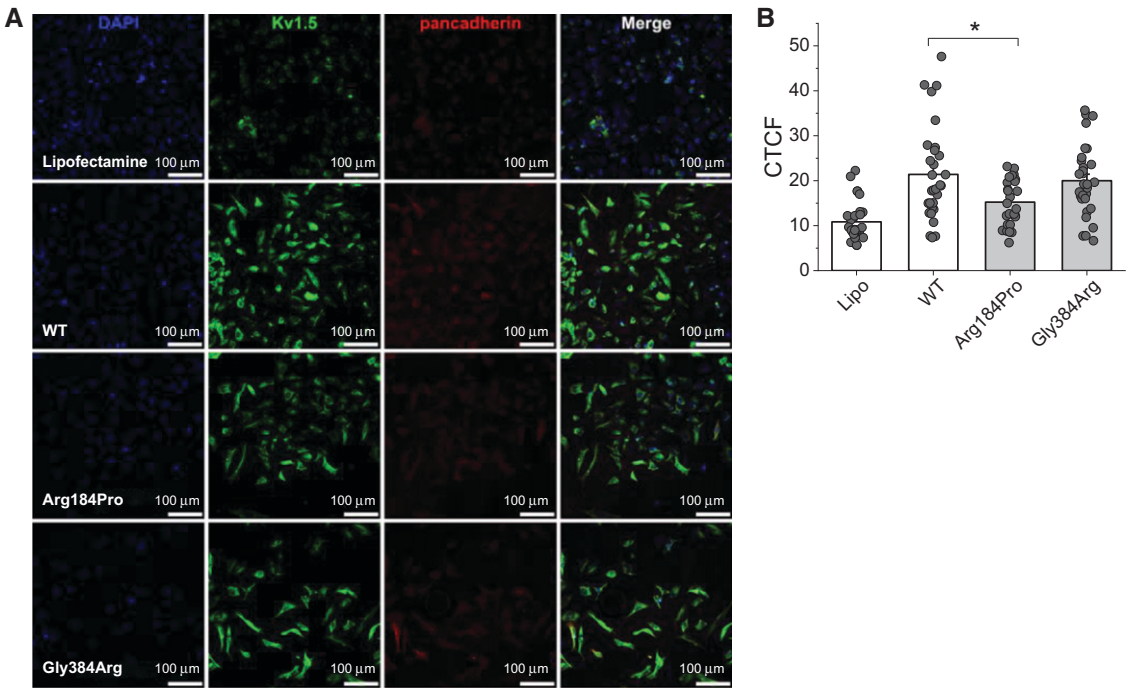

Figure 5. Quantification of *KCNA5* variants after immunofluorescence staining with an anti-Kv1.5 antibody. (*A*) Representative immunofluorescence of HeLa cells that were nontransfected (Lipofectamine; Lipo) or transfected with WT, Arg184Pro, or Gly384Arg channels. Photographs were all taken under the same conditions. Scale bars, 100 μm. (*B*) Kv1.5 fluorescence quantification. Mean fluorescence intensity was quantified for at least 30 cells using ImageJ and expressed as CTCF. Saturated cells were not used for the analysis. Data are presented as mean ± SEM; dots represent single-cell measurements after subtracting the background. *$P < 0.05$. CTCF = corrected total cell fluorescence.

cells transfected with Gly384Arg. These results were confirmed by Western blot (Figures 4B–4D), which revealed the presence of two bands of ~93 and 100 KDa corresponding to the protein formed by Kv1.5 channels plus the GFP (Figure 4B). The upper band corresponds to the fully glycosylated mature channel localized at the plasma membrane, and the lower one corresponds to the core-glycosylated immature form. The expression of the immature form and, especially, the mature form of the channel was reduced in Arg184Pro (Figure 4C). Thus, a clear decrease in the protein maturation process, expressed as percent mature form/total protein, was observed (Figure 4D). *KCNA5* mRNA levels were similar in the WT channel and both variants (*see* Figure E5A), and the transfection and translation efficacy was also similar in the WT channel and Arg184Pro variant. The latter was demonstrated by flow cytometry cotransfecting HEK293 cells with the WT channel or the variant and the pmcherry-N1 plasmid sharing the same cytomegalovirus promoter (Figures E5B–E5D). We found a similar percentage of double-positive (GFP^+ $mCherry^+$) cells and a reduction in the GFP mean intensity as expected, but no differences in the mCherry mean intensity.

In agreement with these data, the immunofluorescence analysis quantifying anti-Kv1.5 fluorescence in the cells confirmed a statistically significant loss of the fluorescent signal in Arg184Pro-transfected ($P < 0.05$), but not in Gly384Arg-transfected cells, compared with the WT channel (Figure 5). Altogether, these data indicated that the Arg184Pro variant affects not only channel gating but also protein expression.

Arg184Pro and Gly384Arg *KCNA5* Variants Decreased Cell Death of hPASMCs

Thereafter, the role of Arg184Pro and Gly384Arg variants in cell apoptosis was evaluated. hPASMCs were transfected with the WT channel or the mutated *KCNA5* channels, and cell viability and apoptosis were analyzed by annexin V and propidium iodide staining. A significant increase in early, late, and total apoptosis was found in hPASMCs transfected with the WT channel compared with nontransfected cells (Figure 6A). As compared with the WT channel, both variants showed reduced apoptotic activity consistent with a significant decrease in both early and late apoptosis and an increase in cell viability (Figures 6B–6D).

Arg184Pro and Gly384Arg Variants Result in Lower SASA of Kv1.5 Channels

Finally, we performed a computational analysis to evaluate the impact of both variants, Arg184Pro and Gly384Arg, in channel gating. For this purpose, the SASA of the Kv1.5 channel was calculated in the WT and both variants. The analysis revealed that both variants presented much lower SASAs compared with the WT channel, consistent with the electrophysiological dysfunctions we had observed (Figure 7).

Clinical Characteristics of *KCNA5* Pathogenic Variants/Cohort Description

There was clinical heterogeneity among the patients carrying the variants analyzed in our study, including five idiopathic PAH types, one sporadic pulmonary venoocclusive

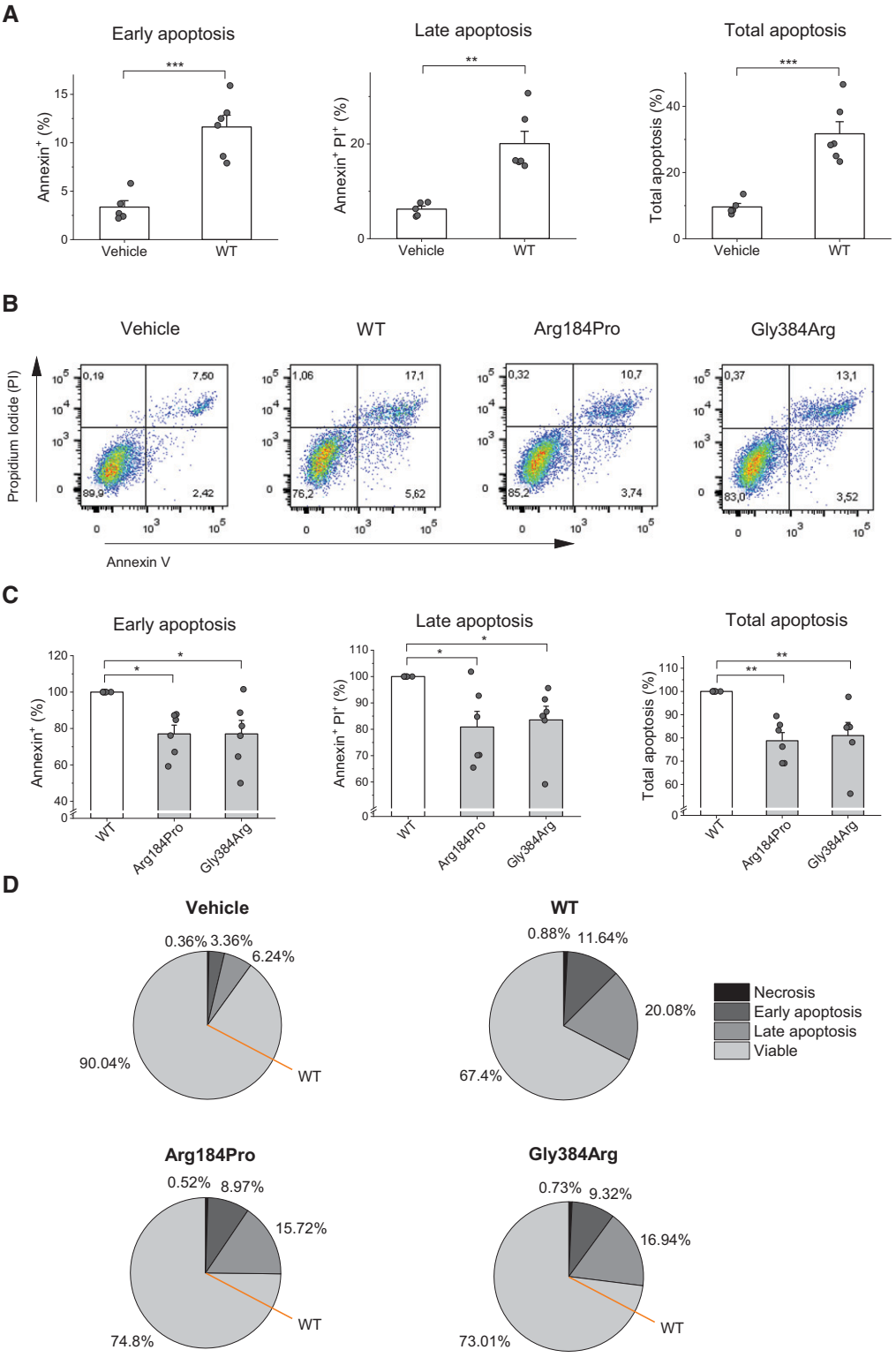

Figure 6. Effects of WT channel and of Arg184Pro and Gly384Arg variants on cell apoptosis in hPASMCs. Annexin V-PI staining was used to evaluate cell viability and apoptosis in hPASMCs 48 hours after transfection. (*A*) Data are presented as percentage of early, late, and total apoptosis over total cells in vehicle and Kv1.5 transfected cells ($n = 6$). (*B*) Representative dot plot of vehicle, WT channel, and Arg184Pro and

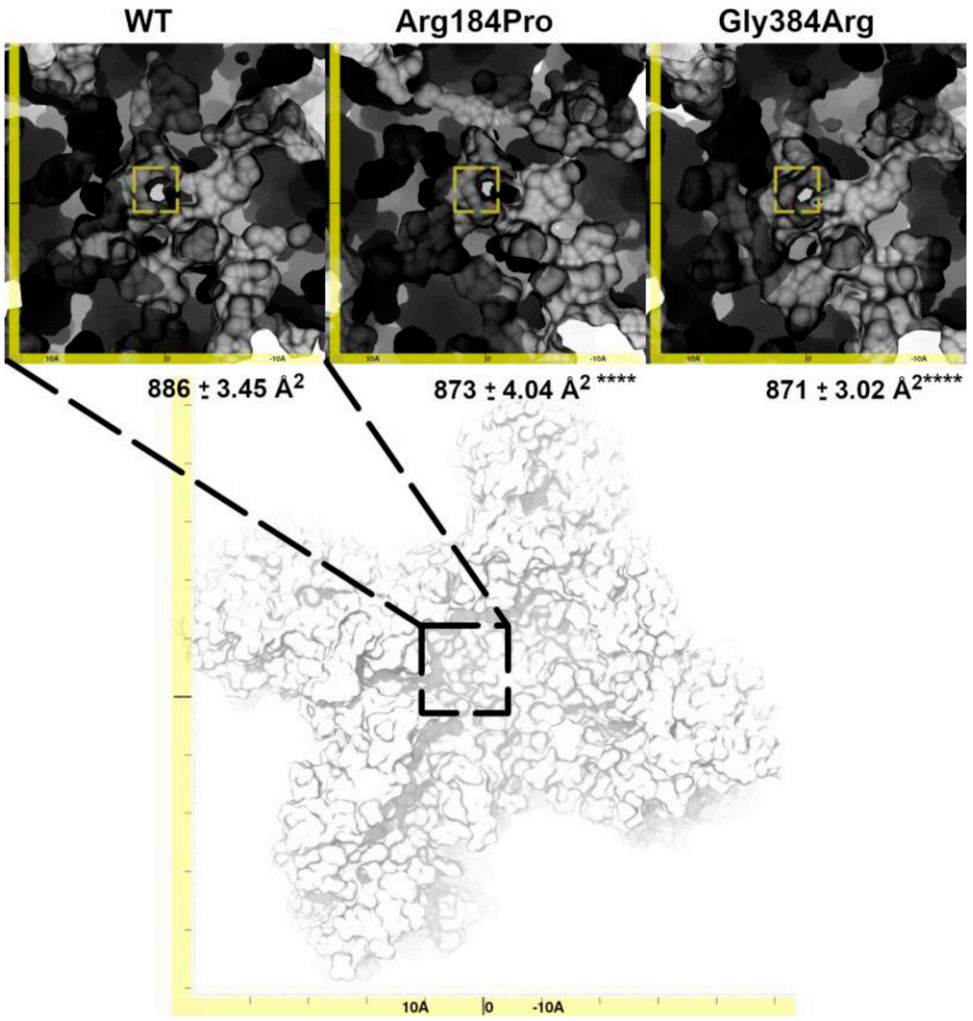

Figure 7. Computational model of WT channel and Arg184Pro and, Gly384Arg variants in Kv1.5 protein. Top view of a representative frame of Kv1.5 WT, Arg184Pro, and Gly384Arg computational models. The solvent-accessible surface area is calculated in each condition. The pore of the channels is highlighted by the square of dashed lines. ****$P < 0.0001$.

disease, and one case with portopulmonary hypertension. Considering those two patients with *KCNA5* pathogenic variants found in our study and the two additional cases with a more dysfunctional gene that we did not analyze, the prevalence of dysfunctional *KCNA5* variants in the entire adult population with PAH genetically tested (475 patients) was ~1%. These patients showed generally an early-onset disease, a female predominance, poor functional status, and high hemodynamic severity (*see* Table E4). Of note, one affected patient experienced repetitive episodes of supraventricular tachycardia, including typical atrial flutter with atypical atrial flutter and atrial fibrillation, and needed an electrophysiological study, in which extensive scarring was observed.

Discussion

In the present study, we have characterized the functional consequences of several *KCNA5* variants found in patients with PAH. Some of these variants (Arg184Pro and Gly384Arg) resulted in a clear loss of potassium channel function. This Kv1.5 channel dysfunction was also associated with impaired apoptosis and enhanced viability of hPASMCs. Our data strengthen the idea that *KCNA5* pathogenic variants may be a risk factor for PAH.

Kv1.5 channel was the first ion channel related to PAH (30). Since then, the association of defective Kv1.5 channels with susceptibility to PAH has been extensively reported in both experimental and clinical

Figure 6. (*Continued*). Gly384Arg variants. (*C*) Data are presented as percentage of early, late, and total apoptosis over Kv1.5 channel in both variants ($n = 6$). (*D*) Pie charts represent the percentage of cells in necrosis, early apoptosis, late apoptosis and viable cells ($n = 6$). In all the panels, results are presented as mean ± SEM. *$P < 0.05$, **$P < 0.01$, and ***$P < 0.001$.

PAH (6, 30). Thus, decreased Kv1.5 channel function has been found in most experimental models of pulmonary hypertension, including the monocrotaline (18), chronic hypoxia (16, 19), and hypoxia-plus-Sugen (11) models, BMPR2 transgenic mice (31), Fawn-hooded rats (17), and 5-HTT–overexpressing mice (11, 32). Impairment of Kv1.5 channel is also found in clinical PAH (30). Most recently, a transcriptomic analysis has confirmed that dysregulation of K^+ channels, including *KCNA5*, is a common hallmark in the different forms of the disease (33).

SNPs in *KCNA5* were first reported by Remillard and colleagues (12). Subsequently, potentially deleterious variants of *KCNA5* were reported in PAH (12, 20, 21, 34, 35) and proposed as a second hit that may lead to early and severe manifestations of the disease (34). However, there is no definitive consensus on its potential pathogenicity, and it is still considered a gene with a low level of evidence as a causal factor (23). Thus, pathogenic variants in this gene remain an unvalidated causal factor, mainly because of the lack of studies assessing their functional consequences (24).

In this study, we selected seven *KCNA5* variants found in a cohort of patients with PAH for functional analysis. Two additional variants were not analyzed, as they encoded truncated or aberrant proteins. We provide a detailed functional analysis of the other seven *KCNA5* variants, which are all localized in the N-terminal domain or loops between the transmembrane segments of the channel (Figure 1A). Kv1.5 current was recorded in cells expressing any of the variants indicating that all formed functional channels. Nevertheless, in two variants (Gly384Arg and especially Arg184Pro), a marked decrease in the Kv1.5 current amplitude and an alteration in channel gating was observed in both time-dependent (kinetics) and voltage-dependent (activation and inactivation curves) electrophysiological characteristics. Moreover, the estimation of single-channel properties by nonstationary noise fluctuation analysis indicated that the reduced activity found in the two variants was associated with decreased single-channel conductance. In line with this, a computational analysis revealed that the SASA in both variants was lower than in the WT channel, which confirms the impact of both mutations on channel gating. We also observed that the Ile356Phe variant showed a slower channel deactivation, whereas the rest of the electrophysiological properties analyzed remain unaffected.

Pousada and colleagues identified the Arg184Pro variant and classified it as pathogenic using different computer algorithms (20). Herein we demonstrate that, indeed, this mutation results in a marked loss of function of the channel. The Arg^{184} residue lies on the T1 domain, which comprises different highly conserved and polar residues that form an interface between the T1 domains of the monomers (29) (*see* Figures E2 and E3). In this case, a positive charged and voluminous amino acid (arginine) is substituted by a nonpolar and small one (proline). The T1 domain is responsible for the tetramerization and governs channel interaction by cytoplasmic regulatory subunits Kvα and Kvβ (29, 36), as well as for plasma membrane expression (37). Deleterious pathogenic variants located in this region have been shown to have important consequences, not only for channel gating but also for protein expression (38). By using cytometry and western blot analyses, we found that the Arg184Pro variant resulted in a strong reduction of Kv1.5 protein. However, these were unrelated to changes in mRNA expression, indicating that the differences found were not due to decreased transcription. To properly reach the plasma membrane and become a mature protein, Kv1.5 channels have to be glycosylated on its extracellular loop between S1 and S2 (39). Thus, the Kv1.5 protein exists in mature and immature forms, which are displayed in two bands on a Western blot. In cells transfected with Arg184Pro, the mature and immature forms of the protein were decreased, as well as the mature/total protein ratio, suggesting that this variant impairs the maturation process. Decreased protein expression of the Arg184Pro variant could be due to augmented degradation, affected tetramerization of the channel, or impaired posttranslational modifications, among other factors. Characterization of the underlying molecular mechanisms and their final impact on cell surface channel expression surely deserve further investigation.

The variant Gly384Arg was described by Castaño and colleagues (22) and classified as a variant with unknown significance according to the ACMG guidelines (40). This variant has been detected in the pseudo–control population database gnomAD with a frequency of $<0.01\%$. Thus, it is considered benign as a causative variant according to the ACMG guidelines. However, given our current functional data, we may consider this as a variant with unknown significance, suggesting that it may have a predisposing rather than a causative role in the pathogenesis of PAH. This variant is located within the S3-S4 loop, substituting a glycine for an arginine (*see* Figure E3). S3-S4 linker length is variable between potassium channel subfamilies and is lower conserved than the T1 (*see* Figure E4). It is interesting to outline that, in Kv1.5 channels, this linker is short and flexible (18 amino acids long) because almost one-third is formed by glycine residues that could be necessary to support the large displacement produced by the S4 movement (41). In fact, previous studies have shown that the extracellular S3-S4 linker is a determinant of activation in various depolarization-activated K^+, Ca^{2+}, and hyperpolarization-activated cyclic nucleotide–gated channels (42–44). Moreover, the positive charge introduced may repel the positive residues of the S4 to such an extent that it affects the correct function of the channel.

No electrophysiological changes were observed in the rest of the *KCNA5* variants analyzed, suggesting a preserved channel function. The unaltered function of two of the variants localized in the S1–S2 linker, Ala287Leu and Pro307Ser, could be expected because the absence of this S1–S2 linkage can generate a functional channel (37). Because our study was performed in an isolated heterologous system (HEK293 cells), we cannot exclude that any of these variants could affect Kv1.5 channel function when expressed in a physiological system because of its modulation by different kinases (PKC, protein kinase A, and tyrosine kinases), as well as by other proteins, such as the Kvβ subunits (45) that are not expressed in HEK293 cells. Thus, our data cannot rule out that the variants that did not affect current amplitude could be modifying the interaction of Kv1.5 with these modulator proteins and indirectly affecting the signaling cascade.

Kv1.5 channels are essential for controlling PASMC membrane potential and regulate many key cellular processes that are dysregulated in PAH, such as contraction, apoptosis, proliferation, and survival (3, 6–9). PAH is characterized by a disruption of the apoptosis/proliferation balance, resulting in enhanced PASMC viability. Brevnova and colleagues showed that *KCNA5* overexpression increases Kv current and

enhances apoptosis in PASMCs, proposing *KCNA5* gene transfer as a strategy to prevent PAH progression (4). In the present work, the Arg184Pro and Gly384Arg variants, which severely affected current amplitude, resulted in a decreased apoptosis of hPASMCs compared with the WT channel, demonstrating that *KCNA5* dysfunction in both variants affects cell viability. Thus, in addition to affecting channel activity, both variants were associated with a clear impairment in a key PASMC process linked to the disease.

PAH pathophysiology is complex with multiple genetic and environmental factors being related to the disease. It is interesting to note that many of these triggers converge in ion channels, including Kv1.5 (6, 7, 46). For instance, Kv1.5 channel expression, trafficking, or activity can be modulated by several proteins encoded by genes already associated with PAH such as *BMPR2* (31), *CAV1* (9, 47), and *NOTCH3* (48). Thus, it would be expected that the impact of *KCNA5* mutations may be exacerbated in patients with genetic/acquired defects in these proteins. It is also reasonable that, in patients harboring mutations affecting other K^+ channels (i.e., *KCNK3*), Kv1.5 dysfunction may further attenuate total K^+ outward currents and facilitate increased vasoconstriction and vascular remodeling. Therefore, and because the presence of several mutations in the same or in different genes is not uncommon (34, 49, 50), it is conceivable that loss-of-function *KCNA5* mutations may modulate disease penetrance in patients carrying other PAH-related gene mutations.

Although the low number of *KCNA5* variant carriers limits their clinical description, the profile of these patients resembles that of the *BMPR2* variant carriers (51). In this work, most of the significant cases were idiopathic and showed an early onset of disease, and the hemodynamic severity was highly remarkable. Nevertheless, the long-term prognosis of these patients was excellent. One of the pathogenic variants was found in a patient with systemic sclerosis–associated PAH, showing a lighter clinical profile in terms of hemodynamic severity. *KCNA5* gene mutations have been linked to the development of rhythm disturbances as well as to QT interval alterations (52). Nevertheless, we found only one case with a long history of atrial arrhythmias among carriers of pathogenic *KCNA5* variants. Further studies should explore the possible relationship between rhythm disorders and PAH in *KCNA5* variant carriers. ■

Author disclosures are available with the text of this article at www.atsjournals.org.

Acknowledgment: The authors thank Carmen Valenzuela and Dirk J. Snyders for providing the wild-type Kv1.5 plasmid; Laura Molero from the Interdepartmental Investigation Service of the Universidad Autónoma de Madrid for her help with the cytometry; and Inés Pazos, Sebastián Comesaña, and Verónica Outeriño from the Centro de Apoio Científico-Técnico á Investigación for their help in imaging and sequencing. The authors also thank the Spanish Consortium of Ion Channel in Pulmonary Hypertension.

References

1. Humbert M, Guignabert C, Bonnet S, Dorfmüller P, Klinger JR, Nicolls MR, *et al.* Pathology and pathobiology of pulmonary hypertension: state of the art and research perspectives. *Eur Respir J* 2019;53:1801887.
2. Stenmark KR, Frid MG, Graham BB, Tuder RM. Dynamic and diverse changes in the functional properties of vascular smooth muscle cells in pulmonary hypertension. *Cardiovasc Res* 2018;114:551–564.
3. Burg ED, Remillard CV, Yuan JXJ. Potassium channels in the regulation of pulmonary artery smooth muscle cell proliferation and apoptosis: pharmacotherapeutic implications. *Br J Pharmacol* 2008;153:S99–S111.
4. Brevnova EE, Platoshyn O, Zhang S, Yuan JXJ. Overexpression of human KCNA5 increases IK V and enhances apoptosis. *Am J Physiol Cell Physiol* 2004;287:C715–C722.
5. George MP, Gladwin MT, Graham BB. Exploring new therapeutic pathways in pulmonary hypertension. Metabolism, proliferation, and personalized medicine. *Am J Respir Cell Mol Biol* 2020;63:279–292.
6. Boucherat O, Chabot S, Antigny F, Perros F, Provencher S, Bonnet S. Potassium channels in pulmonary arterial hypertension. *Eur Respir J* 2015;46:1167–1177.
7. Mondéjar-Parreño G, Cogolludo A, Perez-Vizcaino F. Potassium (K^+) channels in the pulmonary vasculature: implications in pulmonary hypertension. Physiological, pathophysiological and pharmacological regulation. *Pharmacol Ther* 2021;225:107835.
8. Cogolludo A, Villamor E, Perez-Vizcaino F, Moreno L. Ceramide and regulation of vascular tone. *Int J Mol Sci* 2019;20:411.
9. Cogolludo A, Moreno L, Lodi F, Frazziano G, Cobeño L, Tamargo J, *et al.* Serotonin inhibits voltage-gated K+ currents in pulmonary artery smooth muscle cells: role of 5-HT2A receptors, caveolin-1, and KV1.5 channel internalization. *Circ Res* 2006;98:931–938.
10. Hughes FM Jr, Bortner CD, Purdy GD, Cidlowski JA. Intracellular K+ suppresses the activation of apoptosis in lymphocytes. *J Biol Chem* 1997;272:30567–30576.
11. Mondejar-Parreño G, Callejo M, Barreira B, Morales-Cano D, Esquivel-Ruiz S, Moreno L, *et al.* miR-1 is increased in pulmonary hypertension and downregulates Kv1.5 channels in rat pulmonary arteries. *J Physiol* 2019;597:1185–1197.
12. Remillard CV, Tigno DD, Platoshyn O, Burg ED, Brevnova EE, Conger D, *et al.* Function of Kv1.5 channels and genetic variations of KCNA5 in patients with idiopathic pulmonary arterial hypertension. *Am J Physiol Cell Physiol* 2007;292:C1837–C1853.
13. Yuan XJ, Wang J, Juhaszova M, Gaine SP, Rubin LJ. Attenuated K+ channel gene transcription in primary pulmonary hypertension. *Lancet* 1998;351:726–727.
14. Antigny F, Hautefort A, Meloche J, Belacel-Ouari M, Manoury B, Rucker-Martin C, *et al.* Potassium channel subfamily K member 3 (KCNK3) contributes to the development of pulmonary arterial hypertension. *Circulation* 2016;133:1371–1385.
15. Ma L, Roman-Campos D, Austin ED, Eyries M, Sampson KS, Soubrier F, *et al.* A novel channelopathy in pulmonary arterial hypertension. *N Engl J Med* 2013;369:351–361.
16. Hong Z, Weir EK, Nelson DP, Olschewski A. Subacute hypoxia decreases voltage-activated potassium channel expression and function in pulmonary artery myocytes. *Am J Respir Cell Mol Biol* 2004; 31:337–343.
17. Bonnet S, Michelakis ED, Porter CJ, Andrade-Navarro MA, Thébaud B, Bonnet S, *et al.* An abnormal mitochondrial-hypoxia inducible factor-1alpha-Kv channel pathway disrupts oxygen sensing and triggers pulmonary arterial hypertension in fawn hooded rats: similarities to human pulmonary arterial hypertension. *Circulation* 2006;113: 2630–2641.
18. McMurtry MS, Bonnet S, Wu X, Dyck JRB, Haromy A, Hashimoto K, *et al.* Dichloroacetate prevents and reverses pulmonary hypertension by inducing pulmonary artery smooth muscle cell apoptosis. *Circ Res* 2004;95:830–840.
19. Pozeg ZI, Michelakis ED, McMurtry MS, Thébaud B, Wu XC, Dyck JR, *et al.* In vivo gene transfer of the O_2-sensitive potassium channel Kv1.5 reduces pulmonary hypertension and restores hypoxic pulmonary vasoconstriction in chronically hypoxic rats. *Circulation* 2003;107: 2037–2044.
20. Pousada G, Baloira A, Vilariño C, Cifrian JM, Valverde D. Novel mutations in BMPR2, ACVRL1 and KCNA5 genes and hemodynamic parameters in patients with pulmonary arterial hypertension. *PLoS One* 2014;9:e100261.

21. Wipff J, Dieudé P, Guedj M, Ruiz B, Riemekasten G, Cracowski JL, *et al.* Association of a KCNA5 gene polymorphism with systemic sclerosis-associated pulmonary arterial hypertension in the European Caucasian population. *Arthritis Rheum* 2010;62:3093–3100.
22. Castaño JAT, Hernández-Gonzalez I, Gallego N, Pérez-Olivares C, Ochoa Parra N, Arias P, *et al.* Customized massive parallel sequencing panel for diagnosis of pulmonary arterial hypertension. *Genes (Basel)* 2020;11:1158.
23. Morrell NW, Aldred MA, Chung WK, Elliott CG, Nichols WC, Soubrier F, *et al.* Genetics and genomics of pulmonary arterial hypertension. *Eur Respir J* 2019;53:1801899.
24. Southgate L, Machado RD, Gräf S, Morrell NW. Molecular genetic framework underlying pulmonary arterial hypertension. *Nat Rev Cardiol* 2020;17:85–95.
25. Humphrey W, Dalke A, Schulten K. VMD: visual molecular dynamics. *J Mol Graph* 1996;14:33–38, 27–28.
26. Ribeiro JV, Bernardi RC, Rudack T, Stone JE, Phillips JC, Freddolino PL, *et al.* QwikMD—integrative molecular dynamics toolkit for novices and experts. *Sci Rep* 2016;6:26536.
27. Maverick EE, Tamkun MM. High spatial density is associated with non-conducting Kv channels from two families. *Biophys J* 2022;121: 755–768.
28. Kwan DCH, Fedida D, Kehl SJ. Single channel analysis reveals different modes of Kv1.5 gating behavior regulated by changes of external pH. *Biophys J* 2006;90:1212–1222.
29. Minor DL, Lin YF, Mobley BC, Avelar A, Jan YN, Jan LY, *et al.* The polar T1 interface is linked to conformational changes that open the voltage-gated potassium channel. *Cell* 2000;102:657–670.
30. Yuan JXJ, Aldinger AM, Juhaszova M, Wang J, Conte JV Jr, Gaine SP, *et al.* Dysfunctional voltage-gated K+ channels in pulmonary artery smooth muscle cells of patients with primary pulmonary hypertension. *Circulation* 1998;98:1400–1406.
31. Young KA, Ivester C, West J, Carr M, Rodman DM. BMP signaling controls PASMC KV channel expression in vitro and in vivo. *Am J Physiol Lung Cell Mol Physiol* 2006;290:L841–L848.
32. Guignabert C, Izikki M, Tu LI, Li Z, Zadigue P, Barlier-Mur AM, *et al.* Transgenic mice overexpressing the 5-hydroxytryptamine transporter gene in smooth muscle develop pulmonary hypertension. *Circ Res* 2006;98:1323–1330.
33. Perez-Vizcaino F, Cogolludo A, Mondejar-Parreño G. Transcriptomic profile of cationic channels in human pulmonary arterial hypertension. *Sci Rep* 2021;11:15829.
34. Wang G, Knight L, Ji R, Lawrence P, Kanaan U, Li L, *et al.* Early onset severe pulmonary arterial hypertension with 'two-hit' digenic mutations in both BMPR2 and KCNA5 genes. *Int J Cardiol* 2014;177:e167–e169.
35. Zhu N, Pauciulo MW, Welch CL, Lutz KA, Coleman AW, Gonzaga-Jauregui C, *et al.*; PAH Biobank Enrolling Centers' Investigators. Novel risk genes and mechanisms implicated by exome sequencing of 2572 individuals with pulmonary arterial hypertension. *Genome Med* 2019;11:69.
36. Gulbis JM, Zhou M, Mann S, MacKinnon R. Structure of the cytoplasmic beta subunit-T1 assembly of voltage-dependent K+ channels. *Science* 2000;289:123–127.
37. Lamothe SM, Hogan-Cann AE, Li W, Guo J, Yang T, Tschirhart JN, *et al.* The N terminus and transmembrane segment S1 of Kv1.5 can coassemble with the rest of the channel independently of the S1-S2 linkage. *J Biol Chem* 2018;293:15347–15358.
38. Burg ED, Platoshyn O, Tsigelny IF, Lozano-Ruiz B, Rana BK, Yuan JXJ. Tetramerization domain mutations in KCNA5 affect channel kinetics and cause abnormal trafficking patterns. *Am J Physiol Cell Physiol* 2010;298:C496–C509.
39. Shen NV, Chen X, Boyer MM, Pfaffinger PJ. Deletion analysis of K+ channel assembly. *Neuron* 1993;11:67–76.
40. Richards S, Aziz N, Bale S, Bick D, Das S, Gastier-Foster J, *et al.*; ACMG Laboratory Quality Assurance Committee. Standards and guidelines for the interpretation of sequence variants: a joint consensus recommendation of the American College of Medical Genetics and Genomics and the Association for Molecular Pathology. *Genet Med* 2015;17:405–424.
41. Sand R, Sharmin N, Morgan C, Gallin WJ. Fine-tuning of voltage sensitivity of the Kv1.2 potassium channel by interhelix loop dynamics. *J Biol Chem* 2013;288:9686–9695.
42. Gonzalez C, Rosenman E, Bezanilla F, Alvarez O, Latorre R. Periodic perturbations in Shaker K+ channel gating kinetics by deletions in the S3-S4 linker. *Proc Natl Acad Sci USA* 2001;98:9617–9623.
43. Lesso H, Li RA. Helical secondary structure of the external S3-S4 linker of pacemaker (HCN) channels revealed by site-dependent perturbations of activation phenotype. *J Biol Chem* 2003;278: 22290–22297.
44. Nakai J, Adams BA, Imoto K, Beam KG. Critical roles of the S3 segment and S3-S4 linker of repeat I in activation of L-type calcium channels. *Proc Natl Acad Sci USA* 1994;91:1014–1018.
45. Williams CP, Hu N, Shen W, Mashburn AB, Murray KT. Modulation of the human Kv1.5 channel by protein kinase C activation: role of the Kvbeta1.2 subunit. *J Pharmacol Exp Ther* 2002;302:545–550.
46. Jouen-Tachoire TRH, Tucker SJ, Tammaro P. Ion channels as convergence points in the pathology of pulmonary arterial hypertension. *Biochem Soc Trans* 2021;49:1855–1865.
47. McEwen DP, Li Q, Jackson S, Jenkins PM, Martens JR. Caveolin regulates kv1.5 trafficking to cholesterol-rich membrane microdomains. *Mol Pharmacol* 2008;73:678–685.
48. Song S, Babicheva A, Zhao T, Ayon RJ, Rodriguez M, Rahimi S, *et al.* Notch enhances Ca^{2+} entry by activating calcium-sensing receptors and inhibiting voltage-gated K^{+} channels. *Am J Physiol Cell Physiol* 2020;318:C954–C968.
49. Pousada G, Baloira A, Valverde D. Complex inheritance in pulmonary arterial hypertension patients with several mutations. *Sci Rep* 2016;6: 33570.
50. Viales RR, Eichstaedt CA, Ehlken N, Fischer C, Lichtblau M, Grünig E, *et al.* Mutation in BMPR2 promoter: a 'second hit' for manifestation of pulmonary arterial hypertension? *PLoS One* 2015; 10:e0133042.
51. Navas P, Tenorio J, Quezada CA, Barrios E, Gordo G, Arias P, *et al.* Molecular analysis of *BMPR2*, *TBX4*, and *KCNK3* and genotype-phenotype correlations in Spanish patients and families with idiopathic and hereditary pulmonary arterial hypertension. *Rev Esp Cardiol (Engl Ed)* 2016;69:1011–1019.
52. Ni H, Adeniran I, Zhang H. In-silico investigations of the functional impact of KCNA5 mutations on atrial mechanical dynamics. *J Mol Cell Cardiol* 2017;111:86–95.